Chemical Science

ROYAL SOCIETY OF CHEMISTRY

EDGE ARTICLE

View Article Online
View Journal

Cite this: DOI: 10.1039/d5sc08361c

All publication charges for this article have been paid for by the Royal Society of Chemistry

A Polycondensation–depolymerization strategy enables closed-loop recyclable polyoxalates *via* ring-opening polymerization of six-membered cyclic oxalates

Yalei Liu,[a] Zheng Li,[a] Dongfang Zhao,[a] Yong Shen *[b] and Zhibo Li *[ac]

Developing a simple and efficient strategy for the scalable production of closed-loop recyclable polymers from abundant and low-cost feedstocks remains highly desirable. Here, we present a facile "polycondensation–depolymerization" approach for the large-scale synthesis of cyclic 1,2-alkylene oxalates, which undergo controlled ring-opening polymerization to yield high-molecular-weight polyoxalates. The influence of alkyl substituents on the polymerization kinetics, thermodynamics, and material properties was systematically investigated. Remarkably, these polyoxalates can be chemically recycled to their pristine monomers with high purity and yield using sodium glycolate as a catalyst. Furthermore, the polyoxalates exhibit excellent marine degradability, providing a promising strategy to tailor the seawater degradation behavior of polyesters through copolymerization.

Received 29th October 2025
Accepted 19th December 2025

DOI: 10.1039/d5sc08361c

rsc.li/chemical-science

Introduction

The rapid development of synthetic polymers has enabled their widespread applications in almost every area owing to their lightweight, mechanical robustness, low cost, and durability. However, the prevailing "production-use-disposal" paradigm of the linear plastic economy has led to escalating environmental and resource crises. These challenges have stimulated intensive efforts toward a more sustainable circular plastic economy.[1–3] Besides physical recycling, chemical recycling has been a cutting-edge research frontier in both academic and industrial contexts. In particular, polymers with a "monomer–polymer–monomer" closed-loop lifecycle have emerged as a particularly promising solution to address the end-of-life problem of plastics. Such systems allow on-demand depolymerization under mild, energy-efficient conditions to regenerate pristine monomers that can be re-polymerized into polymers of virgin quality.[4–6] Significant progress has been achieved in recent decades in designing polymers with intrinsic closed-loop recyclability, including polyesters,[7–20] polycarbonates,[21–24] polythioesters,[25–33] polyacetals,[34,35] and polyamides.[36–38] Despite these advances, most reported systems rely on tailor-made cyclic monomers that require elaborate, costly, and multistep syntheses, presenting a substantial barrier to broader development. This limitation highlights the urgent need for efficient, conceptually simple strategies to access suitable cyclic monomers from abundant and inexpensive feedstocks.

Among these, a particularly attractive approach is the controlled depolymerization of prepolymers, which can directly furnish cyclic monomers in high purity. A classic example is the depolymerization of low molecular weight (MW) polylactide (PLA), typically obtained from lactic acid polycondensation, to yield cyclic lactide in the presence of appropriate catalysts.[39–41] Inspired by this paradigm, we envisioned a tandem polycondensation–depolymerization strategy to transform readily available oxalates into cyclic alkyl oxalates with diverse substituents. These monomers can undergo ring-opening polymerization (ROP) to produce polyoxalates with intrinsic closed-loop recyclability.

Polyoxalates represent a particularly promising yet underexplored class of sustainable polymers. Their feedstock, oxalic acid or oxalate, can be obtained on a large scale at low cost *via* carbohydrate oxidation or electrochemical CO_2 reduction.[42] In fact, massive oxalic acid/oxalate is already available from industrial processes, warranting various value-added applications. Beyond their accessibility, polyoxalates are especially attractive due to their unique marine degradability, in sharp contrast to widely used biodegradable polymers such as polylactide (PLA) and poly(butylene adipate terephthalate) (PBAT), which degrade extremely slow in seawater.[43–46]

Traditionally, polyoxalates have been synthesized *via* step-growth polycondensation of oxalic acid or oxalates with diols.

[a]*State Key Laboratory of Advanced Optical Polymer and Manufacturing Technology, College of Polymer Science and Engineering, Qingdao University of Science and Technology, Qingdao, 266042, China. E-mail: zbli@qust.edu.cn*

[b]*College of Chemical Engineering, Qingdao University of Science and Technology, Qingdao, 266042, China. E-mail: shenyong@qust.edu.cn*

[c]*State Key Laboratory of Chemical Engineering and Low-carbon Technology, College of Chemical and Biological Engineering, Zhejiang University, Hangzhou, 310058, China. E-mail: zbli@zju.edu.cn*

For example, Miller and Garcia reported a series of polyoxalates from dimethyl oxalate and linear diols using *p*-toluenesulfonic acid catalysis.[47] Wei and co-workers demonstrated kilogram-scale synthesis of poly(ethylene oxalate) (PEOx) by carefully tuning the stoichiometry and reaction conditions.[46] While effective, the polycondensation route demands stringent stoichiometric control, high temperature, and vacuum conditions to achieve high MWs. In contrast, ROP of cyclic monomers offers superior atom economy, excellent control over MW and dispersity (*Đ*), and well-defined chain-end fidelity. Although ROP has been extensively exploited to prepare polyesters, polythioesters, and polycarbonates, yet cyclic oxalates remain largely unexplored. Earliest work by Carothers described the spontaneous polymerization of ethylene oxalate, albeit without systematic characterization.[48] More recently, Melik-Nubarov and co-workers reported the ROP of cyclic propylene oxalate to yield poly(propylene oxalate) with MW up to 30 kDa.[49] Despite these isolated efforts, a systematic exploration of cyclic 1,2-oxalates as ROP monomers as well as the resulting poly(1,2-oxalate)s' structure–property relationships remains lacking. A key barrier is the facile and versatile synthesis of cyclic oxalates with diverse substituents.

Herein, we demonstrate that a tandem polycondensation–depolymerization strategy enables the efficient synthesis of a family of six-membered cyclic 1,2-oxalates directly from commodity oxalates and diols. Low MW poly(1,2-oxalate)s were first prepared by step-growth polycondensation of dimethyl oxalate with 1,2-alkyl diols, followed by selective depolymerization to afford cyclic oxalates. These monomers then underwent ROP to produce high MW poly(1,2-oxalate)s. The polymerization kinetics, thermodynamics, and thermal properties of the resulting materials were systematically investigated. Importantly, the polyoxalates could be selectively depolymerized back into their cyclic monomers in high yield, thereby completing a fully closed-loop "monomer–polymer–monomer" lifecycle. This work introduces a generalizable strategy to access closed-loop recyclable polymers from commodity oxalates and establishes poly(1,2-oxalate)s as a new platform for sustainable polymer design.

Results and discussion

As illustrated in Scheme 1, the step-growth polycondensation of dimethyl oxalate (DMO) and 1,2-propylene diol was conducted using tetrabutyl titanate (TBT) as the catalyst (Fig. S1). Following reported protocol,[50] the reaction was firstly performed at 80 °C for 1 hour under a nitrogen atmosphere. Subsequently, the temperature was raised step-wisely to 110 °C for 1 hour, 140 °C for 2 hours, and 150 °C for 1 hour. The system pressure was then gradually reduced to 50 Pa at 150 °C and maintained for 1–2 hours to remove methanol and excess 1,2-propanediol, driving the reaction equilibrium toward polymerization. Poly(propylene oxlate) (PPOx) with a M_n = 4.1 kDa and 96% yield can easily prepared as prepolymer. Then, the obtained PPOx prepolymer was directly used for depolymerization without further purification. The depolymerization and monomer isolation was combined together by stirring the low MW

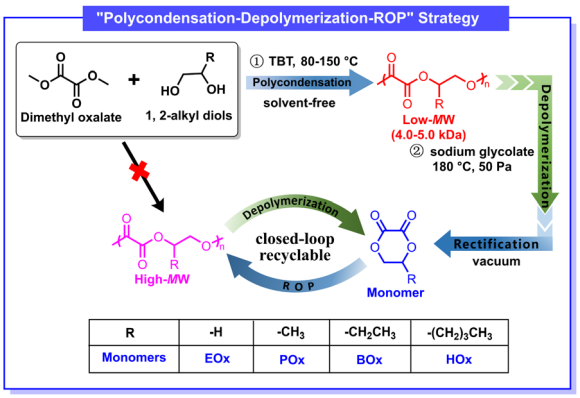

Scheme 1 The preparation of high MW poly(1,2-oxalate)s *via* a "polycondensation–depolymerization" strategy.

PPOx with catalyst at prescribed temperature under reduced pressure, so the POx monomer was directly collected before being subjected to yield and purity measurements. A series of catalysts was then screened for the depolymerization of PPOx, and the results were summarized in Table S1. When 1 wt% stannous octoate ($Sn(Oct)_2$) was used as the catalyst, the depolymerization conducted at 180 °C (~50 Pa) produced POx monomer with 82.9% purity and 63.4% yield. In contrast, both $ZnCl_2$ and *p*-toluenesulfonic acid did not work well as they gave even lower yield and purity (Table S1, runs 2 and 3). When sodium acetate and sodium glycolate were used as the catalyst, the corresponding purity and yield of POx were 83.5%, 87.4% and 86.2%, 90.7%, respectively. We then used strong base KOH as the depolymerization catalyst, and obtained POx monomer with unexpected high purity (93%) and yield (90.2%). We also tried organobase 1,8-diazabicyclo[5.4.0]undec-7-ene (DBU) as the catalyst and found both purity and yield of POx was lower than that of KOH (Table S1, run 7). Apparently, the KOH exhibited best activity and selectivity for the depolymerization of PPOx towards POx monomer. The depolymerization product analyzed by ^{1}H NMR spectrum confirmed the presence of 1,2-propanediol, oligomers and minor unidentified impurities (Fig. S2). After the first round of workout, the crude product was further purified by rectification to afford high-purity POx suitable for ROP with an overall yield of 80%. The molecular structure was unambiguously verified by NMR and electrospray ionization mass spectroscopy (ESI-MS) techniques (Fig. 1a, S2 and S3). It was worth pointing out that the "polycondensation–depolymerization" strategy can be easily scaled up to produce 500 g POx in one batch in the lab, which demonstrated the feasibility of such strategy to make large quantity monomer and also paved a possible roadmap for large scale production of such cyclic monomers.

Since the (de)polymerization thermodynamics and polymer properties can be tailored by introducing suitable substituents on the six-membered ring, we herein synthesized a series of cyclic 1,2-alkylene oxalates, including ethylene oxalate (EOx), 1,2-propylene oxalate (POx), 1,2-butylene oxalate (BOx) and 1,2-hexylene oxalate (HOx) (Scheme 1). By doing so, the impacts of the alkyl length on the properties of resulting poly(1,2-oxalate)s

can be systematically investigated. Several studies have attempted the depolymerization of low MW PEOx but the purity and yield of obtained EOx were not ideal for controlled ROP. On the other hand, the depolymerization of other poly(1,2-oxalate)s was scarcely reported. As such, the preparation of cyclic oxalates *via* the tandem "polycondensation–depolymerization" strategy was first investigated by screening the catalysts and optimizing the conditions (Table S2). BOx and HOx were successfully prepared *via* the similar procedure of POx using corresponding diols as the starting reagents (Table S2, runs 1 and 2).

Three cyclic 1,2-alkylene oxalates were obtained as colorless oil. In contrast, EOx is obtained as a white crystal with a high melting temperature of 144 °C. As such, the depolymerization of PEOx was conducted in a sublimation apparatus at a higher temperature of 210 °C. In such case, when the strong base KOH was used as the depolymerization catalyst, no EOx monomer was collected (Table S2, run 3). When the weaker base sodium glycolate was used as the catalyst, the depolymerization of PEOx afforded EOx with satisfactory yield (60.5%) and purity (85.7%) (Table S2, run 4). The crude EOx was further purified by recrystallization in tetrahydrofuran (THF) to produce high-purity monomer suitable for ROP. The chemical structures of purified cyclic oxalates were verified by NMR and ESI-MS (Fig. S5–S10).

The ROP of the obtained POx was then investigated using a series of catalysts in the presence of benzyl alcohol (BnOH) as the initiator at an initial monomer concentration of 4 mol L^{-1}. The ROP of POx was first attempted using an organophosphazene base *t*Bu-P_2 as the catalyst at 25 °C with a feeding molar ratio of [POx]/[C]/[BnOH] = 300/1/1, which achieved a high monomer conversion of 97% within 2 min but produced PPOx with a moderate molecular weight distribution of $Đ$ = 1.54 (Table S3,run 1). The weaker base *t*Bu-P_1 and DBU also exhibited high catalytic activity but moderate control over the polymerization as supported by the moderate dispersities (Table S3, runs 2 and 3). The typical commercial $AlMe_3$ and TBT showed much lower catalytic activity compared to organobase, achieving low monomer conversion of ~30% at a much longer time of 24 h (Table S3,runs 4 and 5). The rare-earth metal catalyst $La[N(Si(CH_3)_3)_2]_3$ demonstrated extremely high activity, reaching 96% monomer conversion within 1 min and producing PPOx with a $M_{n,SEC}$ of 29.6 kDa (Table S3, run 6). However, the SEC curve of obtained PPOx displayed a shoulder peak (Fig. S11). Additionally, $ZnEt_2$ and MeAl[salen] demonstrated moderate catalytic activity and controllability (Table S3, runs 7–9). For example, the ROP of POx catalyzed by MeAl[salen] reached 95% monomer conversion within 2 h and produced PPOx with a M_n of 32.9 kDa and a moderate $Đ$ of 1.59.

Compared with solution polymerization, solvent-free bulk ROP is more environmentally friendly and suitable for industrial production. Therefore, we then investigated the ROP of POx under bulk condition at 130 °C. The organobases, including *t*Bu-P_1, *t*Bu-P_2, and DBU, still exhibited high catalytic activity, achieving almost quantitative monomer conversion within 2 min. However, significant yellow discoloration of the product was observed, indicating possible side reactions (Table S4, runs 1–3). TBT exhibited much lower catalytic activity and produced PPOx with a much lower M_n compared to the theoretical value (Table S4, run 4). In contrast, $ZnEt_2$, MeAl[salen] and $Sn(Oct)_2$ demonstrated high catalytic activity and good controllability toward the ROP of PPOx (Table S4, runs 5–6 and Table 1, run 1). When $Sn(Oct)_2$ was used as the catalyst, the ROP of POx achieved a monomer conversion of 95% within 20 min. The obtained PPOx had a M_n of 32.3 kDa and a moderate $Đ$ of 1.54 from SEC characterization (Table 1, run 1). Considering its low cost, easy handle and good stability to oxygen and moisture, $Sn(Oct)_2$ was selected as the catalyst for further investigation.

It was found that either decreasing the polymerization temperature to 100 °C or the catalyst loading to [POx]/[$Sn(Oct)_2$]/[BnOH] = 300/0.3/1 did not change the MW and $Đ$ of obtained PPOx, but resulted in a slightly reduced polymerization rate (Table 1, runs 2 and 3). Note that $Sn(Oct)_2$ also exhibited excellent catalytic activity toward the ROP of BOx and HOx, achieving ~94% monomer conversion within 20 min at 130 °C. For example, ROP of BOx conducted at a feeding molar ratio of [BOx]/[$Sn(Oct)_2$]/[BnOH] = 300/1/1 produced PBOx with a M_n = 41.0 kDa and $Đ$ = 1.57 (Table 1, run 4). The resultant PHOx was characterized by SEC to give a M_n = 45.2 kDa and $Đ$ = 1.58 (Table 1, run 5). The measured M_ns agreed well with the theoretical values calculated from the feeding molar ratio and monomer conversion, and the SEC curves were unimodal.

Table 1 Results of ROP of cyclic oxalates catalyzed by $Sn(Oct)_2$ in bulk [a]

Run	Monomer	[M]/[C]/[I]	Temp. (°C)	Time (min)	Conv.[b] (%)	$M_{n,theo}$[c] (kDa)	$M_{n,SEC}$[d] (kDa)	$Đ$[d]
1	POx	300/1/1	130	20	95	37.1	32.3	1.54
2	POx	300/1/1	100	30	92	36.0	32.1	1.56
3	POx	300/0.3/1	130	30	94	36.7	32.2	1.57
4	BOx	300/1/1	130	20	94	40.4	41.0	1.57
5	HOx	300/1/1	130	20	94	48.6	45.2	1.58
6	EOx	300/1/1	180	20	n.d	n.d	n.d	—
7	POx	400/1/1	130	25	95	49.3	37.2	1.60
8	BOx	700/1/1	130	40	93	94.1	71.1	1.59
9	HOx	1000/1/1	130	60	94	162.5	106.6	1.62
10	EOx	1000/1/1	180	60	n.d	n.d	n.d	—

[a] Conditions: 0.02 mmol $Sn(Oct)_2$ was used as the catalyst and benzyl alcohol (BnOH) was used as the initiator. n.d. = not determined due to the poor solubility. [b] Determined by ^1H NMR spectra. [c] Theoretical molecular weight was calculated from the feeding molar ratio and monomer conversion as $M_{n,theo}$ = [M]/[I] × conv.(M) × MW(M) + MW(Initiator). [d] Determined by SEC in THF relative to PS standards.

These results indicated that ROP of cyclic 1,2-alkylene oxalates catalyzed by $Sn(Oct)_2$ exhibited some controlled chain-growth characteristics (Fig. S12). Note all obtained poly(1,2-alkylene oxalate)s were observed as viscous oil at room temperature, indicating their amorphous characteristic and irregular main chain structures. Among these monomers, an exception is EOx. The ROP of EOx was conducted at 180 °C due to the high melting temperature of PEOx (T_m = 172–182 °C). In contrast to the poly(1,2-alkylene oxalate)s that exhibited good solubility in THF, the obtained PEOx was not soluble in common solvents. As an alternative to the SEC characterization, the intrinsic viscosity (IV) of the obtained PEOx was measured using an Ubbelohde viscometer in hexafluoroisopropanol (HFIP) to give a value of 0.80 dL g^{-1} (Table 1, run 6).

The obtained poly(1,2-alkylene oxalate)s were carefully examined with NMR and matrix-assisted laser desorption/ionization time-of-flight mass spectroscopy (MALDI-TOF MS) techniques (Fig. S13–S19). For example, Fig. 1b gives the representative ^{1}H NMR spectrum of PPOx. The characteristic methine (signal b), methylene (signal d), and methyl (signal c) of the repeating units appears at 5.34, 4.43, and 1.42 ppm, respectively. The multiplet observed at 7.38 ppm can be assigned to the phenyl group of BnOH. The molecular weight $M_{n,\,NMR}$ calculated from the relative integral ratio of repeating units (signal b) to the chain-end group (signal a) is 13.2 kDa, which is well consistent with the theoretical value and the measured $M_{n,\,SEC}$ by SEC (Table S8, run 1). The ^{13}C NMR spectrum shown in Fig. S13 also agrees well with the chemical structure of PPOx. Fig. S17 gives the MALDI-TOF mass spectrum of a PPOx sample (M_n = 7.1 kDa, $Đ$ = 1.57) before subjecting to precipitation into methanol. As expected, a major group of molecular ion peaks with a separation of 130.1 Da can be assigned to the linear PPOx initiated by BnOH. Cyclic PPOx is observed in the low MW region due to the intramolecular transesterification or back-biting (Scheme S2, pathway A). In addition, the third group of molecular ion peaks is tentatively assigned to α, ω-phenylmethoxyl capped PPOx while the final group is assigned to 2-hydroxyl-propanoxyl terminated PPOx, which are attributed to the intermolecular transesterification (Scheme S2, pathway B).[51] The MALDI-TOF mass spectra of PBOx and PHOx also exhibit similar four groups of molecular ion peaks due to inter- and intramolecular transesterification (Fig. S18 and S19).

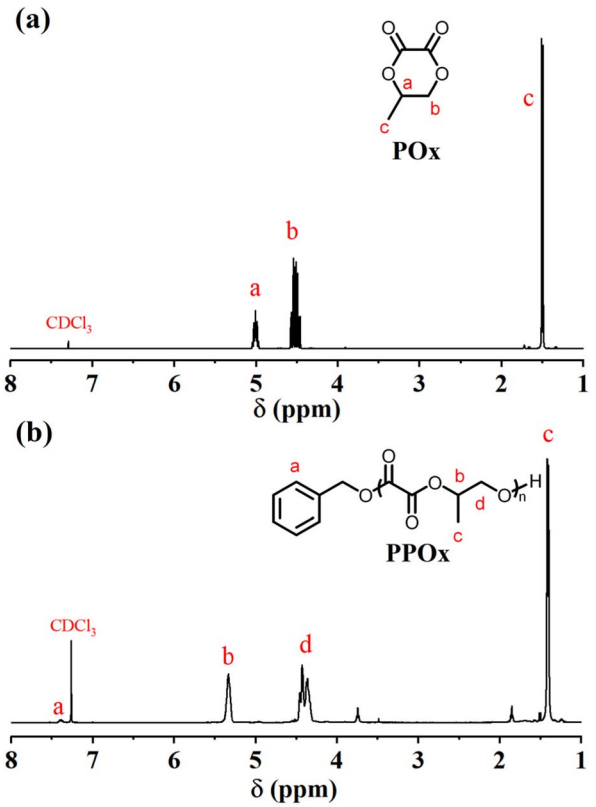

Fig. 1 ^{1}H NMR spectra measured in $CDCl_3$ of (a) POx and (b) PPOx obtained at [POx]/[$Sn(Oct)_2$]/[BnOH] = 100/1/1.

The ROP kinetics of POx, BOx, and HOx were investigated at the molar ratio of $[M]_0/[Sn(Oct)_2]/[BnOH]$ = 300/1/1 in bulk at 130 °C (Fig. 2). The monomer conversions and the M_ns of resultant polyoxalates were monitored by withdrawing aliquots of polymerization mixtures at certain time intervals and measured with ^{1}H NMR and SEC, respectively. The linear correlation of $\ln([M]_0/[M]_t)$ *versus* time for ROP of POx suggested a first-order kinetic behavior relative to the monomer concentration in the presence of $Sn(Oct)_2$ as the catalyst. The apparent kinetic constant calculated from the slope was k_{app} = 0.48 min^{-1}. The ROP of POx exhibited some controlled polymerization characteristics as supported by the good linear dependence of measured M_ns of PPOx as a function of monomer conversions as well as the unimodal SEC traces despite with moderate dispersities (Fig. 2b). Moreover, a series of PPOx with various MWs can be easily prepared by changing the feeding molar ratio of $[M]_0/[BnOH]$. For example, as the targeted degree of polymerization (DP) increased from 100 to 300, the measured M_ns of PPOx linearly increased from 13.2 to 32.2 kDa (Fig. 3). The ROPs of BOx and HOx also exhibited first-order kinetic behaviors, giving a slightly higher k_{app} value of 0.50 and 0.59 min^{-1} compared to that of POx, respectively. Similarly, the controlled polymerization of BOx and HOx catalyzed by $Sn(Oct)_2$ was supported by the linear correlation of measured M_ns of polyoxalates with the monomer conversion (Fig. 2c and d). The M_ns of PBOx and PHOx increased linearly within the range of 500 DP and 700 DP to obtain polyoxalates with M_n up to 60.6 kDa and 94.0 kDa, respectively (Fig. S20 and S21). Note that the minor deviations between $M_{n,theo}$ and $M_{n,SEC}$ were attributed to the transesterification and back-biting side reactions.

It is worth pointing out that high MW polyoxalates can be prepared by further increasing the feeding molar ratio of $[M]_0/[BnOH]$ (Table 1, runs 7–9). For example, when the ROP of POx was conducted at a feeding molar ratio of $[M]_0/[Sn(Oct)_2]/[BnOH]$ = 400/1/1, the M_n of PPOx further increased to 37.2 kDa (Table 1, run 7). PHOx with a M_n up to 106.6 kDa can be obtained at $[M]_0/[Sn(Oct)_2]/[BnOH]$ = 1000/1/1. When the ROP of EOx was conducted at a feeding molar ratio of $[M]_0/[Sn(Oct)_2]/[BnOH]$ = 1000/1/1, a PEOx sample with a IV = 1.56 was obtained. This value is much higher than that of PEOx prepared by polycondensation of DMO and ethylene glycol (IV = 0.78), highlighting the advantage of ROP strategy in preparing high-molecular-weight polyoxalates.[52]

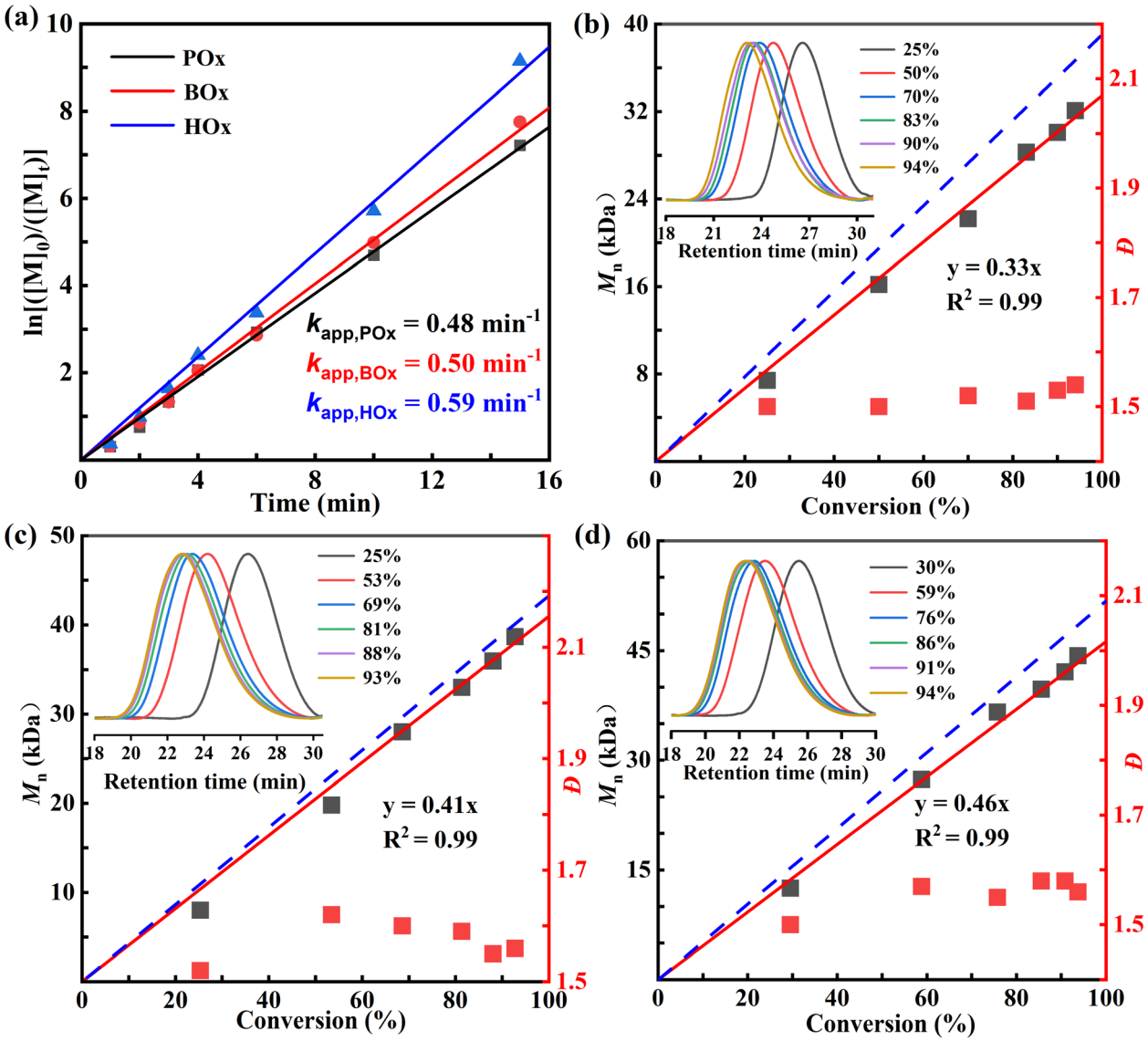

Fig. 2 (a) Kinetic plots of $\ln([M]_0/[M]_t)$ *versus* time at $[M]_0/[BnOH]/[Sn(Oct)_2] = 300/1/1$. Evolution of M_n and $Đ$ of (b) PPOx, (c) PBOx and (d) PHOx as a function of monomer conversion at $[M]_0/[BnOH]/[Sn(Oct)_2] = 300/1/1$. Inset: overlay of SEC curves at different monomer conversion (data shown in Tables S5–S7). The dashed lines indicate the evolution of theoretical molar mass.

We then investigated the polymerization thermodynamics of three monomers (Fig. S22–S24). The ROPs of cyclic 1,2-alkylene oxlates were conducted at different temperatures to measure the equilibrium monomer concentration. The polymerization was considered to reach equilibrium when the monomer conversion measured by ^{1}H NMR remained constant for 30 min. The dependence of the equilibrium monomer concentration ($[M]_e$) on temperature, that is, the Van't Hoff equation $\ln([M]_e) = \Delta H_p^{\theta}/(TR) - \Delta S_p^{\theta}/R$ was used to calculate the thermodynamic parameters, which are summarized in Table 2. For example, the change of enthalpy (ΔH_p^{θ}) and entropy (ΔS_p^{θ}) for ROP of POx was calculated to be −14.1 kJ mol^{-1} and −34.3 J mol^{-1} K^{-1}, respectively, which corresponded to a Gibbs free energy change of $\Delta G_p^{\theta} = -3.87$ kJ mol^{-1} at 25 °C. The ceiling temperature was thus calculated to be 138 °C at an initial monomer concentration of 1 mol L^{-1}. BOx and HOx possessed comparable thermodynamic parameters (ΔH_p^{θ} and ΔS_p^{θ}) with those of POx, which suggested that the length of the alkyl substituents had a negligible impact on their ROP thermodynamics.

The thermal stability of obtained polyoxalates was then investigated with thermogravimetric analysis (TGA). All samples displayed a one-step decomposition profile (Fig. S25). Compared to PPOx ($T_{d,5\%}$ = 193 °C), PBOx and PHOx with longer pendent alkyl groups exhibited improved thermal stability as evidenced by their improved $T_{d,5\%}$ (the temperature at 5% weight loss) of 250 and 257 °C, respectively. The thermal behaviors of obtained polyoxalates were further investigated with differential scanning calorimetry (DSC). No endothermal peaks were observed for PPOx, PBOx and PHOx at both the first and second heating scans. The absence of melting transition

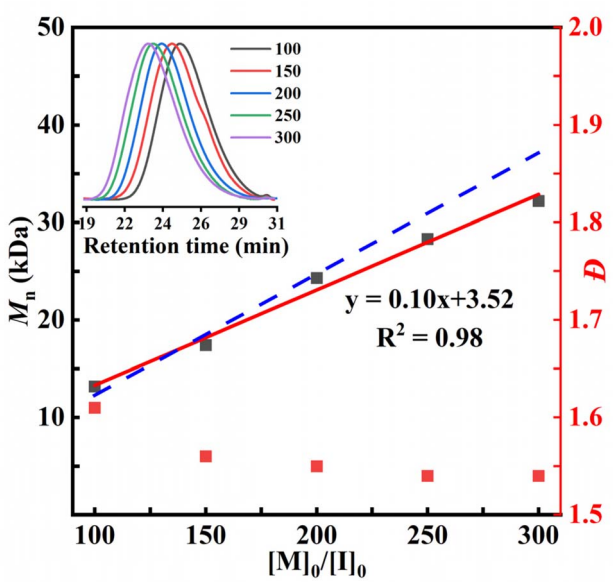

Fig. 3 Evolution of M_n and $Đ$ as a function of $[POx]_0/[BnOH]$ ratio. Inset: overlay of SEC curves at different $[POx]_0/[BnOH]$ ratios ($[BnOH]/[Sn(Oct)_2] = 1:1$, data shown in Table S8). The dashed lines indicate the evolution of theoretical molar mass.

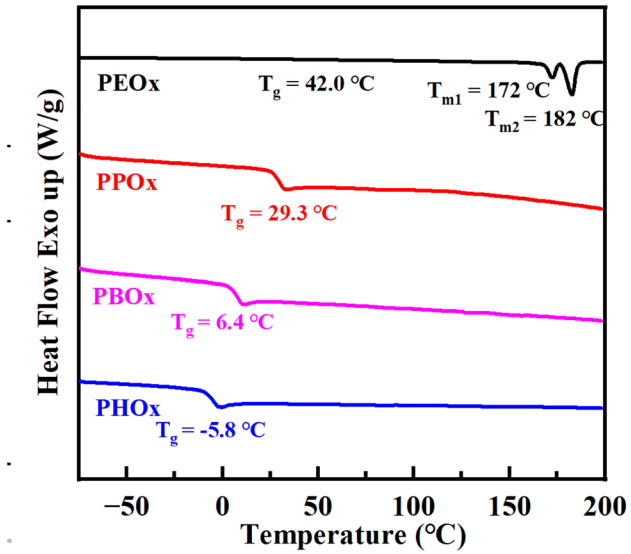

Fig. 4 DSC curves of PEOx, PPOx, PBOx and PHOx sample with a targeted DP of 300.

suggested the amorphous characteristic of poly(1,2-alkylene oxalate)s, which was probably ascribed to the lack of stereoregularity on the polyoxalate backbones. As the pendant alkyl substituent length increased from C1 to C2 to C4, the glass transition temperature (T_g) of PPOx, PBOx, and PHOx slightly decreased from 29.3 to 6.4 to −5.8 °C, respectively (Fig. 4). In contrast, two melting transition peaks at 172 and 182 °C were observed in the second heating scan of DSC curve of PEOx, suggesting that PEOx is a semi-crystalline polyoxalate.

The mechanical properties of obtained PPOx and PEOx were then investigated using uniaxial tensile testing at an extension rate of 50 mm min^{-1}. PBOx and PHOx failed to form films due to their low T_gs and amorphous characteristic, so they were not investigated. Both PPOx and PEOx behaved as brittle plastics and exhibited low enlongation at break. For example, PPOx with a M_n of 37.2 kDa gave a tensile stress of 31.2 ± 1.1 MPa and an elongation at break of 5.4 ± 1.0% at 20 °C. PEOx with a IV = 1.56 exhibited even higher tensile strength of 100.5 MPa, which was 30.5 MPa higher compared to that of PEOx obtained *via* the polycondensation strategy.[52] In sharp contrast to the low degradation rate of PLA and PCL, it is reported that PEOx exhibited rapid degradation in marine environment. We herein compared the hydrolytic degradation behaviors of PEOx and PPOx by immersing their square-shape films in water or artificial seawater. The weigh loss of each sample was monitored by taken out of the specimen from the solution, washed with distilled water and then dried to constant weight. As shown in Fig. 5b, both PEOx and PPOx showed excellent degradability in water and artificial seawater. Compared to PEOx that only achieved 39% degradation in water within 30 days, PPOx demonstrated superior degradability and achieved complete degradation within 5 days. Fig. S27 gives the SEC curves of the remaining polymer during the degradation of PPOx in artificial seawater. As expected, the remaining polymer exhibited a gradually decreased molecular weight but an increased dispersity (Table S15), which was consistent with the random chain scission during hydrolysis. The pH value of the final degradation solution was measured to be 2, suggesting the presence of oxalic acid. Moreover, the ^{1}H NMR spectrum of the solution clearly displays the proton resonances of 1,2-propanediol (Fig. S28). Note that the proton resonances of oxalic acid cannot be observed by ^{1}H NMR spectrum. These results support the good marine degradability of PPOx.

In addition to the low MW polyoxalates, it is supposed that the obtained poly(1,2-alkylene oxalate)s with high MW are also capable of depolymerizing back to pristine monomers given their moderate ceiling temperatures. The depolymerization of PPOx (M_n = 32.2 kDa) that conducted in a distillation apparatus in bulk at 170 °C under reduced pressure (~50 Pa) in the

Table 2 Kinetic and thermodynamic parameters of ROP of cyclic 1,2-alkylene oxlates

M	k_{app} [a] (min^{-1})	ΔH_p^θ (kJ mol^{-1})	ΔS_p^θ (J mol^{-1} k^{-1})	ΔG_p^θ (kJ mol^{-1})	T_c [b] (°C)
POx	0.48 ± 0.01	−14.1 ± 0.6	−34.3 ± 1.4	−3.87 ± 0.73	411 ± 33
BOx	0.50 ± 0.01	−12.9 ± 0.4	−32.0 ± 1.1	−3.48 ± 0.52	403 ± 26
HOx	0.59 ± 0.01	−13.5 ± 0.6	−31.8 ± 1.5	−4.02 ± 0.75	424 ± 38

[a] Conditions: the polymerization was conducted at 130 °C in bulk at $[M]_0/[Sn(Oct)_2]/[BnOH] = 300/1/1$. [b] Calculated at $[M]_0$ = 1.0 mol L^{-1}.

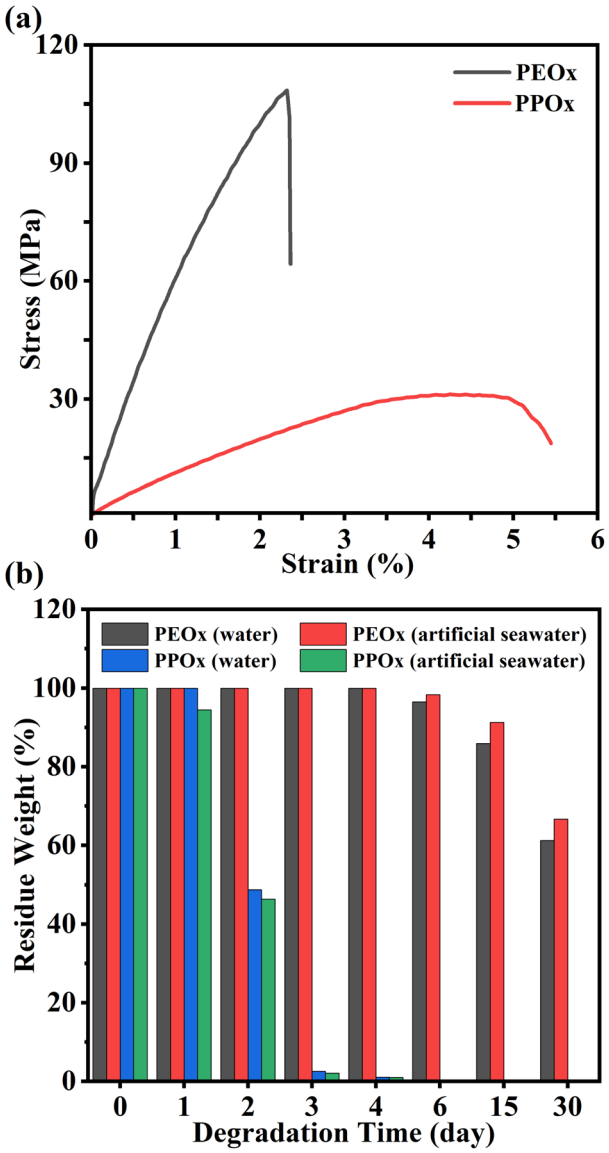

Fig. 5 (a) Stress–strain curves of PPOx (M_n = 37.2 kDa, $Đ$ = 1.60) and PEOx (IV = 1.56). (b) Hydrolytic degradation profiles of PEOx and PPOx in water or artificial seawater.

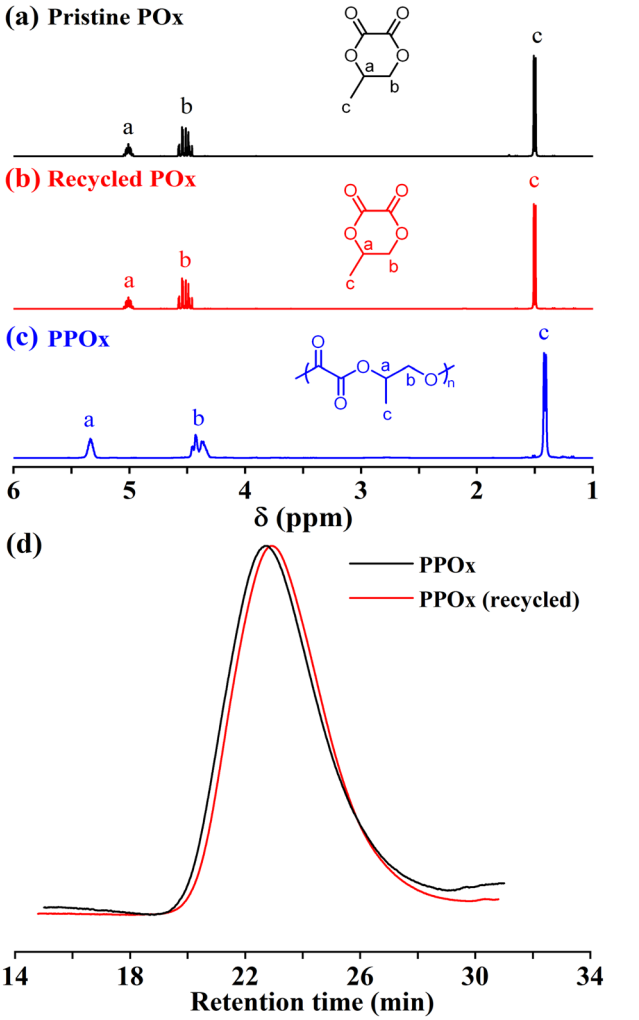

Fig. 6 Overlay of ^{1}H NMR spectra measured in $CDCl_3$ of (a) pristine POx as comparison, (b) recycled POx by vacuum distillation and (c) PPOx prepared from recycled monomer. (d) SEC traces of PPOx prepared from pristine monomer (black line, M_n = 32.2 kDa, $Đ$ = 1.57) and PPOx prepared from recycled monomer (red line, M_n = 29.2 kDa, $Đ$ = 1.58).

presence of 0.5 wt% $Sn(Oct)_2$ as the catalyst produced POx with a yield of 70% within 6 h. The ^{1}H NMR spectrum of recycled POx clearly displayed the signal of $Sn(Oct)_2$ (Fig. S29). This result suggested that $Sn(Oct)_2$ was distilled out from the reaction mixture at such a high temperature and vacuum, which accounted for the moderate monomer yield. In contrast, when 0.5 wt% sodium glycolate was used as the catalyst, the depolymerization of PPOx produced clean POx with an almost quantitative yield of 96% within 4 h under similar conditions. The high-purity of recovered POx was evidenced by the ^{1}H NMR spectrum (Fig. 6b). Of note, the recovered POx can be further repolymerized to produce PPOx with almost the same MW and dispersity as the original monomer (Fig. 6d), thus successfully establishing the "monomer–polymer–monomer" closed-loop life cycle. The successful depolymerization of PBOx and PHOx to recover the monomers was also achieved using sodium glycolate as the catalyst to give a high monomer yield of 90% and 91%, respectively (Fig. S30 and S31).

Conclusions

In summary, we have developed a one-pot "polycondensation–depolymerization" strategy to achieve the scalable production of a series of cyclic 1,2-alkylene oxalate with high yield, which underwent ROPs to produce closed-loop recyclable polyoxalates using $Sn(Oct)_2$ as the catalyst. The ROPs of these cyclic 1,2-alkylene oxalates in the presence of $Sn(Oct)_2$ as the catalyst exhibited first-order kinetic behaviors relative to monomer concentration. The cyclic 1,2-alkylene oxalates exhibited slightly higher kinetic constant as the increase of the alkyl substituent length. On the other hand, the pendant alkyl substituent length had a negligible effect on their polymerization thermodynamic

parameters. The ROPs of cyclic 1,2-alkylene oxalates catalyzed by $Sn(Oct)_2$ exhibited controlled polymerization characteristics as supported by the linear correlation of measured M_ns of obtained polyoxalates as a function of monomer conversion and feeding molar ratio of [M]/[I] despite with moderate dispersities. Compared to the polycondensation strategy, the ROP of cyclic oxalate has a significant advantage in preparing high-molecular-weight polyoxalates. The obtained PPOx, PBOx and PHOx were amorphous polyoxalates with T_g values decreased as their alkyl length increased. In contrast, the high-molecular-weight PEOx sample with an IV = 1.56 was a semi-crystalline polyoxalate and exhibited a high tensile strength of 100.5 MPa but a low enlongation at break of 2.3%. Remarkably, the high MW polyoxalates can be chemically recycled back to recover pristine cyclic oxalates with >90% yield by vacuum distillation at 170 °C in the presence of sodium glycolate as the catalyst. Compared to PEOx, PPOx exhibited superior degradability in both water and artificial sea water. Considering the unique marine degradability of these polyoxalates, it is attractive to further investigate the copolymerization of cyclic oxalates with the commercial lactones or lactides, such as ε-caprolactone and L-lactide, to arbitrarily tune the degradability of obtained copolyesters.

Author contributions

Yalei Liu: investigation, formal analysis, visualization, writing – original draft. Zheng Li and Dongfang Zhao: investigation. Yong Shen and Zhibo Li: conceptualization, formal analysis, supervision, funding acquisition, writing – review & editing.

Conflicts of interest

There are no conflicts to declare.

Data availability

The data supporting this article have been included as part of the supplementary information (SI). Supplementary information: experiment details, ^1H and ^{13}C NMR spectra, ESI-MS spectrum, MALDI-TOF mass spectra, SEC curves, DSC and TGA results, degradation results. See DOI: https://doi.org/10.1039/d5sc08361c.

Acknowledgements

The authors appreciate the financial support by National Natural Science Foundation of China (No. U24A20558 and 52322304), Taishan Scholar Foundation of Shandong Province (No. tsqn202103078), State Key Laboratory of Chemical Engineering and Low-carbon Technology (No. SKL-ChE-25T01).

Notes and references

1 Y. Sun, Z. An, Y. Gao, R. Hu, Y. Liu, H. Lu, X.-B. Lu, X. Pang, A. Qin, Y. Shen, Y. Tao, Y.-Z. Wang, J. Wang, G. Wu, G.-P. Wu, T.-Q. Xu, X.-H. Zhang, Y. Zhang, Z. Zhang, J.-B. Zhu, M. Hong and Z. Li, New sustainable polymers with on-demand depolymerization property, *Sci. China. Chem.*, 2024, **67**, 2803–2841.

2 F. M. Haque, J. S. A. Ishibashi, C. A. L. Lidston, H. Shao, F. S. Bates, A. B. Chang, G. W. Coates, C. J. Cramer, P. J. Dauenhauer, W. R. Dichtel, C. J. Ellison, E. A. Gormong, L. S. Hamachi, T. R. Hoye, M. Jin, J. A. Kalow, H. J. Kim, G. Kumar, C. J. LaSalle, S. Liffland, B. M. Lipinski, Y. Pang, R. Parveen, X. Peng, Y. Popowski, E. A. Prebihalo, Y. Reddi, T. M. Reineke, D. T. Sheppard, J. L. Swartz, W. B. Tolman, B. Vlaisavljevich, J. Wissinger, S. Xu and M. A. Hillmyer, Defining the Macromolecules of Tomorrow through Synergistic Sustainable Polymer Research, *Chem. Rev.*, 2022, **122**, 6322–6373.

3 C. Shi, E. C. Quinn, W. T. Diment and E. Y. X. Chen, Recyclable and (Bio)degradable Polyesters in a Circular Plastics Economy, *Chem. Rev.*, 2024, **124**, 4393–4478.

4 C. Shi, L. T. Reilly, V. S. Phani Kumar, M. W. Coile, S. R. Nicholson, L. J. Broadbelt, G. T. Beckham and E. Y. X. Chen, Design principles for intrinsically circular polymers with tunable properties, *Chem*, 2021, **7**, 2896–2912.

5 X. Tang and E. Y. X. Chen, Toward Infinitely Recyclable Plastics Derived from Renewable Cyclic Esters, *Chem*, 2019, **5**, 284–312.

6 Z. Li, Y. Shen and Z. Li, Ring-Opening Polymerization of Lactones to Prepare Closed-Loop Recyclable Polyesters, *Macromolecules*, 2024, **57**, 1919–1940.

7 C. Li, L. Wang, Q. Yan, F. Liu, Y. Shen and Z. Li, Rapid and Controlled Polymerization of Bio-sourced δ-Caprolactone toward Fully Recyclable Polyesters and Thermoplastic Elastomers, *Angew. Chem., Int. Ed.*, 2022, **61**, e202201407.

8 J. Li, F. Liu, Y. Liu, Y. Shen and Z. Li, Functionalizable and Chemically Recyclable Thermoplastics from Chemoselective Ring-Opening Polymerization of Bio-renewable Bifunctional α-Methylene-δ-valerolactone, *Angew. Chem., Int. Ed.*, 2022, **61**, e202207105.

9 Z. Li, D. Zhao, Y. Shen and Z. Li, Ring-opening Polymerization of Enantiopure Bicyclic Ether-ester Monomers toward Closed-loop Recyclable and Crystalline Stereoregular Polyesters via Chemical Upcycling of Bioplastic, *Angew. Chem., Int. Ed.*, 2023, **62**, e202302101.

10 C. Weng, Z. Ding, W. Qiu, B. Wang and X. Tang, Achieving Exceptional Thermal and Hydrolytic Resistance in Chemically Circular Polyesters via In-Chain 1,3-Cyclobutane Rings, *Angew. Chem., Int. Ed.*, 2024, **63**, e202401682.

11 Q. Yan, J. Ma, W. Pei, Y. Zhang, R. Zhong, S. Liu, Y. Shen and Z. Li, Chemoselective Ring-Opening Polymerization of α-Methylene-δ-valerolactone Catalyzed by a Simple Organoaluminum Complex to Prepare Closed-Loop Recyclable Functional Polyester, *Angew. Chem., Int. Ed.*, 2025, **64**, e202418488.

12 Y. Shen, W. Xiong, Y. Li, Z. Zhao, H. Lu and Z. Li, Chemoselective Polymerization of Fully Biorenewable α-Methylene-γ-Butyrolactone Using Organophosphazene/Urea Binary Catalysts Toward Sustainable Polyesters, *CCS Chem.*, 2021, **3**, 620–630.

13 H. Fan, C. Hu, M. Niu, Q. Zhang, B. Li, X. Pang and X. Chen, Modular Access from Acrylate to a Sustainable Polyester Platform with Large-Span Tunability and Chemical Circularity under Mild Conditions, *J. Am. Chem. Soc.*, 2025, **147**, 9836–9843.

14 C.-T. Han, K. Ma, Z. Zhang, R. W. Clarke, R. R. Gowda, T.-Q. Xu and E. Y. X. Chen, Circular Polymer Designed by Regulating Entropy: Spiro-Valerolactone-Based Polyesters with High Gas Barriers and Adhesion Strength, *J. Am. Chem. Soc.*, 2025, **147**, 4511–4519.

15 H.-Y. Huang, M. Xie, S.-Q. Wang, Y.-T. Huang, Y.-H. Luo, D.-G. Yu, Z. Cai and J.-B. Zhu, Ultratough Thermoplastic Elastomers Based on Chemically Recyclable Cycloalkyl-Substituted Polyhydroxyalkanoates, *J. Am. Chem. Soc.*, 2025, **147**, 7788–7798.

16 Y. M. Tu, X. M. Wang, X. Yang, H. Z. Fan, F. L. Gong, Z. Cai and J. B. Zhu, Biobased High-Performance Aromatic-Aliphatic Polyesters with Complete Recyclability, *J. Am. Chem. Soc.*, 2021, **143**, 20591–20597.

17 L. Zhou, Z. Zhang, C. Shi, M. Scoti, D. K. Barange, R. R. Gowda and E. Y.-X. Chen, Chemically circular, mechanically tough, and melt-processable polyhydroxyalkanoates, *Science*, 2023, **380**, 64–69.

18 J. B. Zhu, E. M. Watson, J. Tang and E. Y. Chen, A Synthetic Polymer System with Repeatable Chemical Recyclability, *Science*, 2018, **360**, 398–403.

19 L. Wang, Y. Shen and Z. Li, Properties Study of Thermoplastic Elastomers Prepared by Sequential Ring-opening Copolymerization of Bio-based δ-Caprolactone and L-lactide, *Acta Polym Sin*, 2024, **55**, 582–593.

20 D. Zhao, Z. Li, Y. Shen and Z. Li, Synthesis and Ring-opening Polymerization of Benzoxy Substituted Oxa-lactones, *Acta Polym Sin*, 2023, **54**, 1303–1311.

21 W. Zhang, J. Dai, Y.-C. Wu, J.-X. Chen, S.-Y. Shan, Z. Cai and J.-B. Zhu, Highly Reactive Cyclic Carbonates with a Fused Ring toward Functionalizable and Recyclable Polycarbonates, *ACS Macro Lett.*, 2022, **11**, 173–178.

22 W.-N. Liu, M. Wang, Z. Ding, Y. Li and B. Wang, Modular Access to Aliphatic Polycarbonates with Tunable Properties and Dual Closed-Loop Recyclability by Polycondensation–Depolymerization–Repolymerization Strategy, *Angew. Chem., Int. Ed.*, 2025, **64**, e202505333.

23 C. Shi, W. T. Diment and E. Y.-X. Chen, Closed-Loop Recycling of Mixed Plastics of Polyester and CO_2-Based Polycarbonate to a Single Monomer, *Angew. Chem., Int. Ed.*, 2024, **63**, e202405083.

24 Y. Yu, B. Gao, Y. Liu and X.-B. Lu, Efficient and Selective Chemical Recycling of CO_2-Based Alicyclic Polycarbonates via Catalytic Pyrolysis, *Angew. Chem., Int. Ed.*, 2022, **61**, e202204492.

25 K. A. Stellmach, M. K. Paul, M. Xu, Y.-L. Su, L. Fu, A. R. Toland, H. Tran, L. Chen, R. Ramprasad and W. R. Gutekunst, Modulating Polymerization Thermodynamics of Thiolactones Through Substituent and Heteroatom Incorporation, *ACS Macro Lett.*, 2022, **11**, 895–901.

26 H.-Z. Fan, X. Yang, J.-H. Chen, Y.-M. Tu, Z. Cai and J.-B. Zhu, Advancing the Development of Recyclable Aromatic Polyesters by Functionalization and Stereocomplexation, *Angew. Chem., Int. Ed.*, 2022, **61**, e202117639.

27 W. Pei, Y. Liu, Q. Yan, K. Yuan, S. Li, Y. Shen and Z. Li, Crystallization/Precipitation Driven Non-equilibrium Ring-opening Polymerization of Thiovalerolactone toward Closed-loop Recyclable Polythioester with Excellent Barrier Properties, *Angew. Chem., Int. Ed.*, 2025, **64**, e202505104.

28 Y. Wang, M. Li, J. Chen, Y. Tao and X. Wang, O-to-S Substitution Enables Dovetailing Conflicting Cyclizability, Polymerizability, and Recyclability: Dithiolactone vs. Dilactone, *Angew. Chem., Int. Ed.*, 2021, **60**, 22547–22553.

29 Y. Zhu, M. Li, Y. Wang, X. Wang and Y. Tao, Performance-Advantaged Stereoregular Recyclable Plastics Enabled by Aluminum-Catalytic Ring-Opening Polymerization of Dithiolactone, *Angew. Chem., Int. Ed.*, 2023, **62**, e202302898.

30 W. Xiong, W. Chang, D. Shi, L. Yang, Z. Tian, H. Wang, Z. Zhang, X. Zhou, E.-Q. Chen and H. Lu, Geminal Dimethyl Substitution Enables Controlled Polymerization of Penicillamine-Derived β-Thiolactones and Reversed Depolymerization, *Chem*, 2020, **6**, 1831–1843.

31 Y. Wang, Y. Zhu, W. Lv, X. Wang and Y. Tao, Tough while Recyclable Plastics Enabled by Monothiodilactone Monomers, *J. Am. Chem. Soc.*, 2023, **145**, 1877–1885.

32 J. Yuan, W. Xiong, X. Zhou, Y. Zhang, D. Shi, Z. Li and H. Lu, 4-Hydroxyproline-Derived Sustainable Polythioesters: Controlled Ring-Opening Polymerization, Complete Recyclability, and Facile Functionalization, *J. Am. Chem. Soc.*, 2019, **141**, 4928–4935.

33 L. Zhou, L. T. Reilly, C. Shi, E. C. Quinn and E. Y. X. Chen, Proton-triggered topological transformation in superbase-mediated selective polymerization enables access to ultrahigh-molar-mass cyclic polymers, *Nat. Chem.*, 2024, **16**, 1357–1365.

34 H. G. Hester, B. A. Abel and G. W. Coates, Ultra-High-Molecular-Weight Poly(Dioxolane): Enhancing the Mechanical Performance of a Chemically Recyclable Polymer, *J. Am. Chem. Soc.*, 2023, **145**, 8800–8804.

35 B. A. Abel, R. L. Snyder and G. W. Coates, Chemically Recyclable Thermoplastics from Reversible-deactivation Polymerization of Cyclic Acetals, *Science*, 2021, **373**, 783–789.

36 X.-T. Tang, J.-A.-Q. Zhou, Y.-M. Tu, H.-Z. Fan, M.-Y. Wang, Q. Cao, Z. Cai and J.-B. Zhu, Ring-Opening Polymerization Enables Access to High-Performance Aliphatic-Aromatic Polyamides with Chemical Recyclability, *Angew. Chem., Int. Ed.*, 2025, **64**, e202505310.

37 R. M. Cywar, N. A. Rorrer, H. B. Mayes, A. K. Maurya, C. J. Tassone, G. T. Beckham and E. Y. X. Chen, Redesigned Hybrid Nylons with Optical Clarity and Chemical Recyclability, *J. Am. Chem. Soc.*, 2022, **144**, 5366–5376.

38 J.-J. Tian, X. Liu, L. Ye, Z. Zhang, E. C. Quinn, C. Shi, L. J. Broadbelt, T. J. Marks and E. Y.-X. Chen, Redesigned Nylon 6 Variants with Enhanced Recyclability, Ductility, and Transparency, *Angew. Chem., Int. Ed.*, 2024, **63**, e202320214.

39 C. F. Gallin, W.-W. Lee, J. A. Byers and A. Simple, Selective, and General Catalyst for Ring Closing Depolymerization of Polyesters and Polycarbonates for Chemical Recycling, *Angew. Chem., Int. Ed.*, 2023, **62**, e202303762.

40 W. Zhao, Z. Guo, J. He and Y. Zhang, Solvent-Free Chemical Recycling of Polyesters and Polycarbonates by Magnesium-based Lewis Acid Catalyst, *Angew. Chem., Int. Ed.*, 2025, **64**, e202420688.

41 T. M. McGuire, A. Buchard and C. Williams, Chemical Recycling of Commercial Poly(L-lactic acid) to L-Lactide Using a High-Performance Sn(II)/Alcohol Catalyst System, *J. Am. Chem. Soc.*, 2023, **145**, 19840–19848.

42 M. A. Murcia Valderrama, R.-J. van Putten and G.-J. M. Gruter, The potential of oxalic – and glycolic acid based polyesters (review). Towards CO_2 as a feedstock (Carbon Capture and Utilization – CCU), *Eur. Polym. J.*, 2019, **119**, 445–468.

43 Q. Luan, H. Hu, X. Jiang, C. Lin, X. Zhang, Q. Wang, Y. Dong, J. Wang and J. Zhu, Melt polycondensation of poly (butylene oxalate-co-succinate) with great potential in curbing marine plastic pollution, *J. Hazard. Mater.*, 2023, **457**, 131801.

44 Q. Luan, H. Hu, X. Ouyang, X. Jiang, C. Lin, H. Zhu, T. Shi, Y.-L. Zhao, J. Wang and J. Zhu, New modifications of PBAT by a small amount of oxalic acid: Fast crystallization and enhanced degradation in all natural environments, *J. Hazard. Mater.*, 2024, **465**, 133475.

45 Z. Tu, L. Wang, Y. Lu, Y. Li, L. Sang, Y. Zhang and Z. Wei, Rapid marine degradable poly(butylene oxalate) by introducing promotion building blocks, *J. Hazard. Mater.*, 2024, **462**, 132791.

46 Z. Tu, Y. Lu, L. Sang, Y. Zhang, Y. Li and Z. Wei, Kilogram-Scale Preparation of Poly(ethylene oxalate) toward Marine-Degradable Plastics, *Macromolecules*, 2023, **56**, 3149–3159.

47 J. J. Garcia and S. A. Miller, Polyoxalates from biorenewable diols via Oxalate Metathesis Polymerization, *Polym. Chem.*, 2014, **5**, 955–961.

48 W. H. Carothers, J. A. Arvin and G. L. Dorough, Studies on polymerization and ring formation. V. glycol esters of oxalic acid, *J. Am. Chem. Soc.*, 1930, **52**, 3292–3300.

49 N. P. Iakimov, E. M. Budynina, A. K. Berkovich, M. V. Serebryakova, V. B. Platonov, E. O. Fomin, A. G. Buyanovskaya, I. V. Mikheev and N. S. Melik-Nubarov, Polymerization of six-membered propylene oxalate, *Eur. Polym. J.*, 2024, **220**, 113410.

50 L. Wang, Z. Tu, J. Liang, Y. Wang and Z. Wei, Development of poly(butylene oxalate-co-furanoate) copolymers with enhanced sustainability and hydrolytic degradability, *J. Hazard. Mater.*, 2024, **480**, 135997.

51 N. P. Iakimov, E. M. Budynina, E. O. Fomin, A. A. Egorova, A. K. Berkovich, M. V. e. Serebryakova, I. D. Grozdova and N. S. Melik-Nubarov, End-group analysis to characterize the ring-opening polymerization of propylene oxalate, *Mendeleev Commun.*, 2025, **35**, 586–588.

52 Z. Tu, Y. Lu, Y. Zhang, Y. Li and Z. Wei, Development of poly(n-alkylene oxalate)s toward a new kind of seawater degradable plastics, *Mater. Today Sustainability*, 2023, **22**, 100378.